Available online at www.sciencedirect.com
ScienceDirect
Journal of Non-Crystalline Solids xxx (2006) xxx–xxx
JOURNAL OF NON-CRYSTALLINE SOLIDS
www.elsevier.com/locate/jnoncrysol

Viscosity and glass transition temperature of hydrous float glass

P. Del Gaudio [a,*], H. Behrens [a], J. Deubener [b]

[a] Institut für Mineralogie, Universität Hannover, D-30167 Hannover, Germany
[b] Institut für Nichtmetallische Werkstoffe, TU Clausthal, D-38678 Clausthal-Zellerfeld, Germany

Received 28 November 2006

Abstract

Viscosity of water-bearing float glass (0.03–4.87 wt% H_2O) was measured in the temperature range of 573–1523 K and pressure range of 50–500 MPa using a parallel plate viscometer in the high viscosity range and the falling sphere method in the low viscosity range. Melt viscosity depends strongly on temperature and water content, but pressure up to 500 MPa has only minor influence. Consistent with previous studies on aluminosilicate compositions we found that the effect of dissolved water is most pronounced at low water content, but it is still noticeable at high water content. A new model for the calculation of the viscosities as a function of temperature and water content is proposed which describes the experimental data with a standard deviation of 0.22 log units. The depression of the glass transition temperature T_g by dissolved water agrees reasonably well with the prediction by the model of Deubener [J. Deubener, R. Müller, H. Behrens, G. Heide, J. Non-Cryst. Solids 330 (2003) 268]. Using water speciation measured by near-infrared spectroscopy we infer that although the effect of OH groups in reducing T_g is larger than that of H_2O molecules, the difference in the contribution of both species is smaller than predicted by Deubener et al. (2003). Compared to alkalis and alkaline earth elements the effect of protons on glass fragility is small, mainly because of the relatively low concentration of OH groups (max. 1.5 wt% water dissolved as OH) in the glasses.

Keywords: Glass transition; Pressure effects; FTIR measurements; Alkali silicates; Silicates; Soda-lime-silica; Fragility; Viscosity; Water in glass

1. Introduction

Water is the most abundant volatile dissolved in magmas as well as in industrial silicate glasses. It is well known that even small amounts of dissolved water have a tremendous effect on melt viscosity. The effect of water on melt viscosity is more pronounced than the effect of any other volatiles as well as the effect of alkali oxides [2]. Previous studies already showed a large decrease of viscosity when small amounts of H_2O were incorporated in the melt and a continued but less pronounced decrease in viscosity as the melt becomes increasingly water-rich [3,4]. It is likely that this trend is related to the speciation of water in the melt. IR and NMR spectroscopic measurements on hydrous glasses demonstrate that at low water content (0.1 wt%), H_2O is mainly dissolved as OH groups whereas at high water content (>4 wt%) molecular H_2O is the predominant hydrous species [5,6]. The water speciation measured in glasses reflects the equilibrium speciation at the glass transition temperature [7,8]. In situ spectroscopy at high temperature gives evidence that molecular H_2O is a stable species in the melt above its liquidus, but its relative abundance decreases with increasing temperature [9].

Viscosities of commercial or technical glasses (container, soda-lime-silica glass or float glass) at ambient pressure are well characterized both in the high viscosity and in the low

* Corresponding author. Present address: Istituto Nazionale di Geofisica e Vulcanologia, Department of Seismology and Tectonophysics – High Pressure High Temperature Laboratory of Experimental Volcanology and Geophysics, I-00143 Rome, Italy. Tel.: +39 06 51860380/230; fax: +39 06 51860507.
E-mail address: delgaudio@ingv.it (P. Del Gaudio).

0022-3093/$ - see front matter © 2006 Published by Elsevier B.V.
doi:10.1016/j.jnoncrysol.2006.11.009

viscosity range [10–15]. Most of the studies, however, do not yield information to which extent variations of total water content C_w expressed in wt% (chemically dissolved as hydroxyl groups and physically dissolved as molecular water) can affect the melt viscosity. Studies on the effect of dissolved water on melt viscosity focussed mainly on aluminosilicates with compositions relevant for natural processes [3,16–24]. Systematic investigations on water-bearing silicate glasses relevant for industrial glass composition are missing. Industrial glasses melted with air/gas or air/oil flame typically contain 0.028–0.035 wt% water, when melted with oxycombustion the water content may reach 0.045–0.065 wt% [1]. Hydrous glasses containing several wt% of H_2O can be produced by fusion in high pressure apparatuses [25,26].

Viscosity measurements on hydrous low viscosity melts can only be carried out at elevated pressures because otherwise the melt will rapidly degas. The falling sphere method is the only established technique for measurement of viscosity of water-rich melts at viscosities below 10^6 Pa s [4,17] (through our paper we will use Pa s as viscosity units, 1 Pa s = 10 poise). Near the glass transition it is often possible to measure viscosity of water-rich melts even at ambient pressure because the duration of viscosity experiments is short compared to the time required for significant diffusion of water out of the melt [3,16,20,21,27]. However, measurements are restricted to temperatures of at most a few tenth degrees above the glass transition. When approaching the softening point (temperature at which the viscosity of the melt is $10^{6.6}$ Pa s), the glasses rapidly start to foam. Foaming can be depressed when using a high pressure parallel plate viscometer, but surface hardening of the viscosity sample by diffusive dehydration of the melts become a severe problem [17]. The difficulties to investigate hydrous glasses, especially with several weight percent of H_2O, make the knowledge of viscosities of water-bearing glass more uncommon.

In the present study we have chosen a commonly used technical float glass to investigate systematically the effect of dissolved water on melt viscosity. One of our goals is to establish a model for determination of viscosity as function of temperature, pressure, and water content. To extend the existing viscosity dataset (which includes primarily anhydrous float glass data), we provide a set of viscosity data for H_2O-bearing float glass melts (from 0.03 wt% to 4.87 wt%) under pressure (from 50 MPa to 500 MPa) in a wide range of temperature (from 593 K to 1523 K). Combining the new viscosity data with water speciation measured here and by Stuke et al. [6] allows us to test the three-component model proposed by Tomozawa et al. [28] and refined by Deubener et al. [1]. This model predicts the glass transition temperature of water-bearing glasses, T_g, as a weighted combination of different limiting glass transition temperatures related to dry glass, hydroxyl groups, and molecular water. Finally, the effect of dissolved water on the fragility of silicate melts will be discussed on the basis of our new results.

2. Experimental method

2.1. Sample preparation

Technical glass beads from *Potters-Ballotini company (Kirchheimbolanden, Germany)* was used for the investigation of the effect of water on melts viscosity. The composition of re-melted glass beads measured by electron microprobe using the wavelength dispersive analysis (72.01 SiO_2, 0.76 Al_2O_3, 0.10 Fe_2O_3, 3.92 MgO, 8.96 CaO, 13.13 Na_2O, 0.25 K_2O in wt%, see [26]) matches that of typical float glass.

Hydrous samples, with the total water content in the range of 0.03–4.87 wt%, were synthesized by high pressure re-melting of glass beads mixed with distilled water in Pt capsules. To minimize the pore volume and achieve good compaction of glasses, fractions of glass spheres with diameters of 0–50 μm, 100–200 μm, and 490–620 μm were mixed in a ratio of 1:1:1 for 10–15 min with a shaking machine. Platinum capsules with an inner diameter of 6 mm and a length of 30–40 mm were used for the synthesis of the samples. The capsules were first welded at the bottom then filled stepwise with powder and water. To achieve a fully compact filling of the Pt capsule each powder layer was compressed by a steel piston before inserting water. Finally, the capsules were sealed by arc welding to the top while the lower part of the capsules were cooled in water or with a tissue moistened with water and frozen in liquid nitrogen in order to avoid any evaporation of water during the sealing. To test for leakage, the capsules were weighed before and after annealing at 383 K for at least 60 min.

The synthesis of hydrous glasses was then carried out in an internally heated pressure vessel (IHPV) for at least 24 h at a temperature of 1523 K and under a pressure range of 200–500 MPa. Argon gas was used as pressure medium. Temperature was measured with four K-type thermocouples and controlled by a Eurotherm type 900 programmed controller with a precision of ±5 K, while pressure was measured by a strain gauge manometer to a precision of ±5 MPa.

Each run was terminated by switching off the heating power while the pressure was maintained constant by automatic pumping. The initial cooling rate was about 200 K/min decreasing to about 100 K/min in the range of glass transition. This was fast enough to avoid crystallization in all samples resulting in a bubble- and crystal-free glass.

2.2. Determination of water content

2.2.1. Karl-Fischer titration (KFT)

The water content of water-rich glasses was measured after thermal dehydration using Karl-Fischer titration (KFT) of the released H_2O [26]. For each analysis a single piece of glass was used instead of ground glass in order to minimize the contribution of absorbed water on the glass surface. The glasses pieces were inserted in the apparatus

Please cite this article in press as: P. Del Gaudio et al., Viscosity and glass transition temperature of hydrous float glass, J. Non-cryst. Solids (2006), doi:10.1016/j.jnoncrysol.2006.11.009

within a Pt crucible. The sample was heated using a fast ramp by stepwise increasing the power of the high frequency generator. A temperature of more than 1273 K was reached after 3–4 min and the titration was finished usually after 5–8 min. The final temperature was close to 1550 K. To account for unextracted water, values of 0.17 ± 0.04 wt% for glasses containing less than 1.5 wt% of H_2O and 0.13 ± 0.04 wt% for glasses with higher water content were added to the measured KFT values. These corrections are based on soda-lime-silica glasses and float glasses studied by [26].

2.2.2. IR spectroscopy

Slices were cut from the raw material after synthesis and also after experiments, for several samples, from the cylinder along the major axis. The slices were doubly polished and then analyzed by IR microspectroscopy. Thickness (40–1000 μm) was measured using a Mitutoyo micrometer with a precision of ±2 μm. Depending on water content, absorption spectra of the sections were recorded in mid-infrared (MIR) or near infrared (NIR) using a Bruker IRcopeII IR microscope connected to an FTIR-spectrometer Bruker IFS 88. Measurement conditions for MIR were: globar light source, KBr beam splitter, narrow range MCT detector, 50 scans for sample and background and a spectra resolution of 2 cm^{-1}. Measurement conditions for NIR were: tungsten light source, CaF_2 beam splitter, narrow range MCT detector, 100 scans for sample and background and a spectra resolution in the order of 4 cm^{-1}.

The total H_2O content of glasses having lower water content than 2.5 wt% can be measured using mid-infrared bands at 3550 cm^{-1} and 2850 cm^{-1} caused by OH^- stretching vibrations of weakly and strongly H-bonding water species, respectively. The peak height (absorbance) of the MIR bands was determined by subtracting a background absorbance measured at 4000 cm^{-1} from the absorbance at the peak maximum. The practical absorption coefficient ε_{pract} (defined by assuming that a single band of a complex IR spectrum reflects the total water) is less sensitive to the water content for the 2850 cm^{-1} band than for 3550 cm^{-1} band in float glass [26]. Therefore, ε_{2850} was preferred for the determination of water content. It is noteworthy, however, that at very low water contents (<0.02 wt%) the band at 2850 cm^{-1} becomes less suitable for water determination because of high relative intensity of superimposed network vibration bands [29]. The water content of glasses with expected water contents above 2.5 wt% was measured using the combination bands of OH groups at 4500 cm^{-1} and H_2O molecules at 5200 cm^{-1}. The tangent to the curve was chosen as baseline [6].

The concentration of the water species and the total water content were calculated by the peak height of absorption bands with the Lambert–Beer law [26]:

$$C_i = \frac{1801.5 \cdot A_i}{\rho \cdot d \cdot \varepsilon_i}. \quad (1)$$

A_i is the absorbance of i-band, ρ is the density of the glass (g/L), d is the thickness (cm) of the sample and ε_i the absorption coefficient (L mol^{-1} cm^{-1}) of each i-band. When using the MIR bands, C_i corresponds to the total water content C_w (in wt%). In case of the near infrared bands at 4500 cm^{-1} and at 5200 cm^{-1}, C_i is the concentration of water dissolved as OH groups and H_2O molecules, respectively, and the total water content is obtained by summing up both concentrations. Density of float glasses with different water contents was calculated after [26] as ρ (in g/L) $= (2505 \pm 4) - (14.8 \pm 0.8) \cdot C_w$. The following absorption coefficients (in L mol^{-1} cm^{-1}) were used in the calculations: $\varepsilon_{2850} = 40.2 \pm 2.4$ [26], $\varepsilon_{4500} = (0.497 \pm 0.004) + (0.051 \pm 0.002)$ C_w and $\varepsilon_{5200} = 0.89 \pm 0.06$ [6]. The total H_2O content measured on the water-bearing float glass ranges between 0.03 and 4.87 wt% (see Tables 1a and 1b).

2.3. Viscosity measurements

2.3.1. High viscosity range

Near the glass transition the viscosity was measured under pressure using a parallel plate viscometer operating in an IHPV (internally heated pressure vessel) [30]. The expression for the determination of the viscosity (Pa s) is the following equation [30–32].

Table 1a
MIR spectroscopy on float glass

Sample	Thickness (cm)	Density (g/L)	A_{2850}	C_w IR (wt%)	C_w KFT (wt%)
FG0a	0.0499	2505	0.085	0.03 ± 0.01	–
FG1	0.1366	2505	0.335	0.04 ± 0.01	–
FG2	0.0200	2505	0.073	0.06 ± 0.01	–
FG3	0.0200	2503	0.179	0.16 ± 0.02	–
FG4	0.0200	2502	0.214	0.19 ± 0.02	–
FG6	0.0140	2501	0.220	0.28 ± 0.03	–
FG9 (i)	0.0119	2493	0.353	0.53 ± 0.05	0.66 ± 0.08
FG9 (f)	0.0093	2493	0.350	0.68 ± 0.03	–
FG10	0.0046	2491	0.239	0.93 ± 0.14	0.84 ± 0.16
FG11	0.0070	2487	0.479	1.23 ± 0.05	1.07 ± 0.14
FG12	0.0067	2479	0.662	1.79 ± 0.18	1.52 ± 0.07
FG13	0.0078	2474	0.919	2.14 ± 0.10	2.05 ± 0.08

Please cite this article in press as: P. Del Gaudio et al., Viscosity and glass transition temperature of hydrous float glass, J. Non-cryst. Solids (2006), doi:10.1016/j.jnoncrysol.2006.11.009

Table 1b
NIR spectroscopy on float glass

Sample	Thickness (cm)	Density (g/L)	A_{4500}	A_{5200}	C_{OH} (wt%)	C_{H_2O} (wt%)	C_w *IR* (wt%)	C_w KFT (wt%)
FG7	0.1003	2501	0.024	–	0.33 ± 0.04	–	0.33 ± 0.04	–
FG8	0.1012	2498	0.051	–	0.68 ± 0.03	–	0.68 ± 0.03	0.50 ± 0.09
FG14(i)	0.0381	2468	0.049	0.058	1.47 ± 0.06	1.26 ± 0.08	2.72 ± 0.09	2.47 ± 0.07
FG14(f)	0.0385	2468	0.048	0.059	1.43 ± 0.12	1.26 ± 0.07	2.70 ± 0.14	–
FG15(i)	0.0393	2440	0.056	0.135	1.47 ± 0.11	2.86 ± 0.07	4.33 ± 0.13	3.66 ± 0.12
FG15(f)	0.0376	2440	0.051	0.092	1.48 ± 0.15	2.02 ± 0.09	3.50 ± 0.17	–
FG16(i)	0.0411	2450	0.060	0.135	1.52 ± 0.10	2.72 ± 0.09	4.24 ± 0.13	–
FG16(f)	0.0379	2450	0.054	0.134	1.46 ± 0.14	2.93 ± 0.09	4.39 ± 0.16	–
FG17(i)	0.0379	2446	0.056	0.160	1.46 ± 0.10	3.50 ± 0.10	4.96 ± 0.14	–
FG17(f)	0.0388	2446	0.056	0.146	1.46 ± 0.13	3.11 ± 0.11	4.57 ± 0.17	–
FG18(i)	0.0384	2443	0.054	0.166	1.39 ± 0.10	3.57 ± 0.10	4.96 ± 0.14	4.66 ± 0.14
FG18(f)	0.0391	2443	0.056	0.163	1.42 ± 0.10	3.45 ± 0.07	4.87 ± 0.13	–

Notes: (i) refers to the initial water content and (f) to the final water content. Absorption coefficients used in the evaluation of the NIR bands are taken from [6]. Density was calculated after [26].

$$\eta = \frac{M \cdot g \cdot (L_0 - \Delta L_0)}{3 \cdot S_0 \cdot L_0 \cdot \left(\frac{\Delta \ln L}{\Delta t}\right)}, \quad (2)$$

where η is the viscosity (Pa s), M is the mass of the weight loaded on top of a cylindrical glass sample (g), g is acceleration of gravity (9.81 m/s^2), L_0 is initial length of the sample (m), ΔL_0 is the change in length during the experiment, S_0 the initial surface, L is the length of the sample at time t.

A buoyancy correction is needed because the mass of the load M was determined at ambient pressure while the viscometer operates under higher argon pressure (the minimum was 50 MPa and maximum 400 MPa). Assuming the temperature at the load as 323 K, the density of argon at a given pressure (in MPa) was calculated according to [33] as $\rho_{(T=323\ K)} = 0.3824 \cdot \ln P - 0.8518$. Variation in temperature at the load by ±25 K affects the calculated viscosity by less than 0.003 log units. The effective weight of the load under pressure is given as [30]

$$W_P = W_R - \frac{W_R \cdot \rho_{Ar}}{\rho_L}, \quad (3)$$

where W_P is the weight of the load under pressure and W_R at ambient pressure (1033 g), ρ_{Ar} is density of argon at experimental pressure and ρ_L is density of the load (8.103 g/cm^3). The weight of the load decreases from 1033 g at ambient pressure to 849 g at 400 MPa assuming a temperature of 323 K.

For all viscosity experiments, the sample temperature and thermal gradient along the sample was determined using the melting point of zinc (increasing from 692 K at ambient pressure to 705 K at 400 MPa) [34] or tin (increasing from 505 K at 0.1 MPa to 524 K at 400 MPa) [35]. The first step of the experiments was the pressurization of the vessel up to 200 MPa. Then three different consecutive ramps (40, 5, and 40 K/min) were applied to reach the temperature for first viscosity measurement. The second ramp with lower rate covers the temperature range near the melting point of the metal used for T calibration. The starting temperature for viscosity measurement was estimated so that the viscosity was approximately $10^{11.5}$ Pa s. Temperature was maintained for 30 min to allow thermal expansion and mechanical relaxation of the viscometer.

When the thermal conditions were stable and the deformation rate did not vary with the time, small temperature increases by ±5–10 K followed by dwells of ≈10–15 min were used to measure viscosities. This dwell time was sufficient to get steady state deformation (constant viscosity) (Fig. 1). Most experiments were run at 200 MPa, but in some cases the pressure was varied in the order 200, 300, 100, 50, 200 MPa. As shown in Table 2 in most of the experiments the first viscosity measurement was repeated at the end of the sequence in order to verify the reproducibility of the viscosities (see Tables 2 and 3).

2.3.2. Low viscosity range

Low viscosity data were measured by using the falling-sphere method. This method requires the determination of the exact position of the sphere in the glass cylinder before and after the experiment. A cylinder with diameter of 4–6 mm was cored from the raw water-bearing glass and cut perpendicular to the major axis in two cylindrical parts, a longer one (almost 10 mm) and a smaller one (1–2 mm). The remaining glass was crushed as powder.

The smaller piece of glass was placed on bottom of a platinum capsule which was closed at one end with a platinum cup (in order to get a container with cylindrical shape). Then a small amount of Pt powder (<1 μm in diameter) was strewed onto the glass piece to serve as a marker for distance measurement. Next the longer cylinder was inserted in the capsule and was covered with a small amount of the glass powder. A platinum or palladium sphere was placed on top of the glass powder at the center of the capsule and covered with glass powder. The top of the capsule was then sealed by arc-welding while cooling the sample as described above. The spheres used in this study were made from strands of Pt or Pd wire (thickness = 2.5 10^{-4} cm) twisted together and melted by a sudden DC current. This method produces spheres with small radius (radius of 45–80 μm), suitable for these experiments.

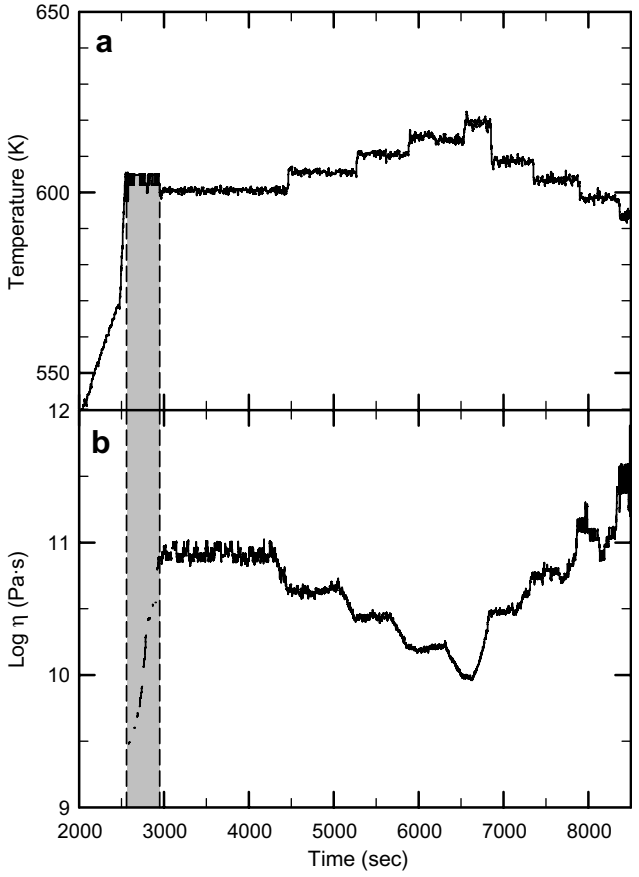

Fig. 1. Viscosity data obtained during a sequence of creep experiments at 200 MPa (FG18, 4.87 wt% H_2O). (a) Variations in temperature and (b) variations in logarithm of viscosity. Note that the apparent increase in viscosity after reaching the first temperature plateau is due to relaxation of the viscometer.

The capsules were placed in an IHPV and ran at 1523 K and 200–500 MPa for few minutes to pre-melt the whole glass assemblage. The cylinders were then removed from the capsule and the position of the sphere with respect to the marker layer was determined. This was accomplished using an optical microscope equipped with an x–y stage. The glass cylinder was immersed in oil with a similar refraction index as the glass (1.622) to improve the visibility of the sphere. This position was used as the starting position for the subsequent viscosity experiment. The sample was then cleaned in acetone, dried at ambient temperature, and sealed again within a platinum capsule.

The procedure for the viscosity experiments was as follows: The capsules were loaded into the IHPV, pressure was increased to the desired pressure, and then the sample was heated firstly with 30 K/min to 1023 K and then with 70 K/min or 100 K/min to the target temperature. The duration of the experiments was in the range of 5 min to 1 h depending on the experiment viscosity. At the end of the experiment the capsules were quenched, by shutting of heating power, with an initial rate of the order of 200 K/min. The quenching freezes the sphere in place and the distance the sphere has travelled during the experiment can be measured, using the microscope and immersion oil technique mentioned earlier and a scaled micrometer. Terminal velocity was determined from the distance covered and time of travel. Viscosity can be calculated using Stokes' law [17]:

$$\eta = \frac{2 \cdot g \cdot r^2 \cdot (\sigma - \rho)}{9 \cdot \upsilon} \cdot C_F, \tag{4}$$

where η is the viscosity, g acceleration of gravity, r radius of the sphere, σ density of the sphere (21.45 g/cm^3 the Pt sphere and 12.02 g/cm^3 the Pd sphere at room temperature), ρ density of molten glass, υ terminal velocity of the sphere, and C_F is Faxen correction that take in account the effect of viscous drag by the capsule wall on the settling sphere. Density of melt at experimental condition was calculated after [36] using the partial molar volume of water after [37].

In short term experiments there could be a significant contribution to the total descent of the sphere during heating and cooling. To consider the movement of the sphere before and after reaching the target temperature T_{target} the effective run duration t_{eff} was calculated in the same way as it is done for diffusion experiments, [38]

$$t_{eff} = \int \exp\left[\frac{-E_a}{R} \cdot \left(\frac{1}{T} - \frac{1}{T_{target}}\right)\right] \cdot dt, \tag{5}$$

where E_a is the activation energy (kJ/mol) and R is the gas constant. The underlying idea is that the viscosity ratio $\eta(T_{target})/\eta(T)$ scales the time which is required to achieve the same falling distance of the sphere at T_{target} and at T. For instance, in a melt containing 0.33 wt% H_2O (sample FG7, Table 4) the sphere needs only 1/11 of the time to reach the same falling distance at 1523 K ($\log\eta = 1.54$, average of two measurements) than at 1323 K (calculated $\log\eta = 1.56$). For simplicity an Arrhenian temperature dependence of viscosity is assumed in Eq. (5). We are aware that viscosity is not necessarily Arrhenian over a wide range of temperature but for a narrow T-range the assumption of linear variation of viscosity with reciprocal temperature is a good approximation. Calculations show that only the last 300 K below the target temperature contributes significantly to the effective run duration and, thus, application of temperature-independent E_a value appears to be justified (compare Fig. 6). The activation energy for viscous flow depends strongly on water content especially for low H_2O contents [17] and hence E_a needs to be determined for the specific water content of the sample. To estimate E_a firstly we calculated the Vogel–Fulcher–Tammann (VFT) parameters by combining the falling sphere data based on the dwell time with the results of the creep experiment with a melt of similar water content. Next, the average activation energy was determined for the temperature interval of 300 K below the target temperature. The so-obtained values of E_a vary from 215 ± 6 at 0.33 wt% H_2O to 101 ± 5 kJ/mol at 4.39 wt% H_2O. The resulting increase of run time ranged from 38 to 115 s. Using samples with relatively high H_2O content (FG15 and FG16 see Table 4) the

Table 2
Results of creep experiments at 200 MPa

T (K)	Logη (Pa s)	T (K)	Logη (Pa s)	T (K)	Logη (Pa s)	T (K)	Logη (Pa s)
FG0a, 0.03 wt% (f)		FG1, 0.04 wt% (f)		FG2, 0.06 wt% (f)		FG3, 0.16 wt% (f)	
851	10.72	850	10.89	831	10.89	821	10.82
870	10.09	861	10.31	852	10.55	842	10.32
881	9.74	869	9.95	862	10.16	852	9.96
892	9.40	881	9.64	872	9.79	862	9.64
902	9.09			882	9.47	873	9.31
911	8.75			891	9.15	882	8.99
				901	8.85	892	8.66
				881	9.49	864	9.59
				870	9.82	824	10.54
				861	10.22		
				841	10.64		
FG4, 0.19 wt% (f)		FG6, 0.28 wt% (f)		FG9, 0.53 wt% (i)–0.68 wt% (f)		FG10, 0.93 wt% (f)	
821	10.84	848	9.49	770	11.41	813	8.49
831	10.45	819	10.52	775	11.02	762	10.29
841	10.08	809	10.90	780	10.90	771	10.01
851	9.79	799	11.23	791	10.48	781	9.65
862	9.46	789	11.65	801	10.17	763	10.45
872	9.15	827	10.25	811	9.84	762	10.58
883	8.86	827	10.26	820	9.51		
821	10.72	846	9.57	804	10.09		
				775	10.99		
FG11, 1.23 wt%		FG12, 1.79 wt%		FG13, 2.14 wt%		FG14, 2.72 wt% (i)–2.70 wt% (f)	
731	10.76	722	9.77	690	10.63	667	11.19
721	11.17	702	10.83	699	10.15	677	10.67
741	10.41	692	11.19	709	9.73	683	10.48
751	10.07	712	10.24	699	10.12	688	10.41
761	9.75	722	9.90	689	10.56	694	10.21
772	9.41	732	9.51	684	10.91	699	9.99
732	10.73	742	9.11	702	10.07	705	9.73
793	8.68	722	9.78	723	9.26	696	10.07
		702	10.61			675	10.90
		719	9.97			656	11.75
		718	9.89				
FG15, 4.33 wt% (i)–3.50 wt% (f)		FG16, 4.24 wt% (i)–4.39 wt% (f)		FG17, 4.96 wt% (i)–4.57 wt% (f)		FG18, 4.96 wt% (i)–4.87 wt% (f)	
624	11.45	600	11.70	601	11.35	605	10.91
635	10.77	610	11.16	611	10.80	609	10.63
646	10.31	622	10.41	621	10.19	615	10.43
650	10.07	627	10.17	632	9.74	619	10.20
656	9.86	632	9.92	642	9.26	623	9.98
661	9.60	636	9.69	626	9.90	614	10.47
665	9.37	641	9.45	616	10.46	609	10.76
656	9.77	630	9.91	601	11.33	602	11.04
645	10.21	620	10.46			593	11.51
635	10.82	611	11.36				
625	11.39						

Notes: (i) refers to the initial water content and (f) to the final water content.

run time for falling sphere experiment had to be very short, in the order of 4–5 min. As a consequence, viscosity data have a relatively large error (see Table 4). Major sources of error in addition to the time correction are the settling distance (measured using a scaled micrometer with a resolution of ± 10 μm), measurements of the sphere radius (measured using a scaled micrometer with an error of the measurement of the radius of 1–5 μm), and temperature of the sample (precision of the temperature is ± 10 K).

3. Experimental results

3.1. Water content of glasses

Pre- and post-experiment water contents agree, within the error range, in all cases but one (FG15), indicating no significant water loss during the experiments. The concentration profiles of two float glasses containing 0.28 wt% and 2.14 wt% of H_2O show no significant water

Please cite this article in press as: P. Del Gaudio et al., Viscosity and glass transition temperature of hydrous float glass, J. Non-cryst. Solids (2006), doi:10.1016/j.jnoncrysol.2006.11.009

Table 3
Results of creep experiments with variation of pressure

T (K)	P (MPa)	Log η (Pa s)
FG1, 0.04 wt%		
861	300	10.50
861	350	10.54
861	100	10.46
861	200	10.31
FG13, 2.14 wt%		
702	300	10.19
702	400	10.07
702	100	10.21
702	50	10.20
702	200	10.07
FG4, 0.28 wt%		
790	300	11.71
819	300	10.73
847	300	9.64
777	100	11.78
798	100	11.16
817	100	10.47
837	100	9.76
794	50	11.30
813	50	10.55
831	50	9.89
850	50	9.23
846	200	9.57
FG10, 0.93 wt%		
771	300	10.14
771	400	10.17
771	100	10.08
771	50	10.14
771	200	10.01

loss after viscosity experiments (Fig. 2(a) and (b)). At most a rim of 20 μm in thickness was affected by dehydration. Negligible water loss during creep experiment is evidenced also by the high reproducibility of viscosity data within one experiment. Two examples of water-rich melts are shown in Fig. 3(b). After adjusting the same temperature as in the beginning of the sequence the viscosities agree within 0.1 log units. The final water content of the sample FG15 of 3.50 wt% is smaller than the value of 4.33 wt% measured with IR spectroscopy after the falling sphere experiment and then an experiment using viscometer. As the initial water content measured by KFT (3.66 wt% of H_2O) agrees well with the value measured after high viscosities experiment, we attribute the high value of 4.33 wt% to inhomogeneous distribution of water in the glass batch (only a small glass fragment at the end of the sample was used for IR spectroscopy).

3.2. Creep experiments

Operating with the creep apparatus allows collection of multiple viscosity data from each experiment (Table 2 and 3). Typically 10 min are sufficient to reach steady state conditions (constant viscosity) after changing temperature or pressure (Fig. 1). In Fig. 3(b) the viscosity data for two water-rich float glasses (3.50 and 4.57 wt%) are shown. In both experiments the scatter in the data with respect to the Arrhenius curve is within ±0.08 log units, which is comparable to the reproducibility of ±0.05 log units reported by Schulze et al. [30] for measurements on dry melts. At the end of the experiment samples were returned to the starting temperature to verify whether or not viscosity at the beginning and at the end of the experiment were consistent. In the two examples shown in Fig. 3(b) the first measurement was reproduced at the end within ±0.02 log units (FG17, 4.60 wt% H_2O) and ±0.06 log units (FG15, 3.57 wt% H_2O). From these results it is concluded that in the range of time (more than 2 h) necessary for these experiments water loss was negligible. IR measurements after experiments support this conclusion (see Fig. 2(a) and (b)).

Comparisons with literature data are possible only for ambient pressure and dry glass. In Fig. 3(a) the viscosities of float glasses (ranging between 0.03 and 4.87 wt% H_2O) measured at 200 MPa (this work) are compared with viscosities calculated at 0.1 MPa after [14,15,39]. Although denoted as soda-lime-silica glass, the samples used by Prado [14,15] are of similar chemical composition (differences of oxides content range between 0.5 wt% for SiO_2

Table 4
Condition and results of falling sphere experiments

Sample	C_w (wt%)	T (K)	P (MPa)	Sphere radius r (μm)	Faxen correction C_F[a]	t_{dwell} (s)	$t_{effective}$ (s)	Falling distance (cm)	Log η (Pa s)
FG7	0.33	1523	200	(Pt)80 ± 2.5	0.89	470	551	0.330	1.57 ± 0.21
FG7	0.33	1523	200	(Pt)80 ± 2.5	0.88[b]	280	361	0.249	1.50 ± 0.21
FG8	0.68	1523	500	(Pt)80 ± 2.5	0.93	415	486	0.520	1.36 ± 0.20
FG8	0.68	1523	500	(Pt)80 ± 2.5	0.74[b]	310	381	0.435	1.24 ± 0.20
FG9	0.68	1523	200	(Pd)45 ± 1.0	0.83	4500	4571	0.857	1.17 ± 0.12
FG9	0.68	1473	200	(Pd)45 ± 1.0	0.93[b]	3600	3638	0.220	1.71 ± 0.12
FG15	3.50	1523	500	(Pd)73 ± 2.5	0.95	300	415	0.981	0.54 ± 0.28
FG16	4.39	1473	500	(Pd)53 ± 1.0	0.86	240	333	0.578	0.78 ± 0.36

Notes: The target temperature was reached using two ramps. In the case of FG7 and FG8 the ramps were of 30 °C/min to 800 °C and 100 °C/min to the target T. For FG9, FG15 and FG16 the two ramps used were: 30 °C/min to 800 °C and 70 °C/min to the target T.

[a] Faxen correction is calculated as described in [17]. Different values of C_F for second runs with same samples [b] originate from different horizontal displacement of the sphere relative to the sample axis. The minimum distance of the sphere to the capsule wall is used in the calculation of C_F.

[b] Second experiment with the same sample as described in the row above.

Please cite this article in press as: P. Del Gaudio et al., Viscosity and glass transition temperature of hydrous float glass, J. Non-cryst. Solids (2006), doi:10.1016/j.jnoncrysol.2006.11.009

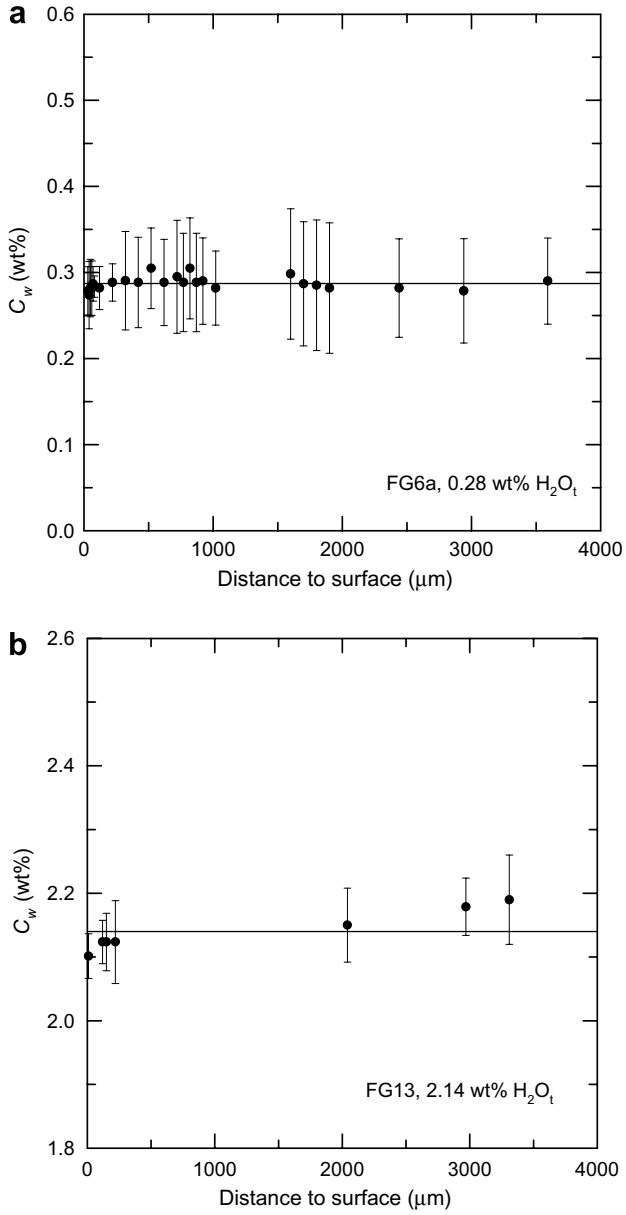

Fig. 2. Examples of water concentration-distance profiles measured after creep experiments in glasses with two different water contents.

to 0.6 wt% in the case of MgO) as used in our study (same manufacturer) and, hence, the data are directly comparable. The same is valid for the so called *window glass* used in [10,39]. Deviations between the viscosities of our melt containing 0.03 wt% of water and the data of [39] are within ±0.08 log units except for the viscosity measured at 851 K (deviation of ±0.18 log units). Agreement with Prado et al. [14,15] is also well (Fig. 4).

When dissolving water in the melt, the viscosity strongly decreases (Fig. 4). For instance adding 4.87 wt% of water to the dry melt reduces the temperature at which the viscosity of float glass equals 10^{10} Pa s by 252 K. The effect of water is more pronounced at low than at high water content.

3.3. Falling sphere experiments

To verify the reliability of the falling sphere method, two experiments were duplicated at the same pressure and temperature with samples FG7 (0.33 wt% H_2O) and FG8 (0.68 wt% H_2O) varying the run duration. The viscosity of FG7 sample was calculated from two different measured displacements at 1523 K and pressure of 200 MPa. First an experiment with an effective run duration of 551 s was carried out and then another one with 361 s. The difference between the two viscosities was 0.07 log units, which is less then the estimated experimental error, see Table 4. Duplicated measurements with sample FG8 agree within ±0.08 log units which is significantly lower than the experimental error. These experiments demonstrate that steady state velocity is established in these experiments and the errors introduced by the acceleration and deceleration of the spheres are negligible.

Fig. 4 presents a plot with the results of viscosity (expressed as logarithm of viscosity) versus water content (expressed as weight percent of H_2O). The data of nominally dry melt were calculated from VFT parameters published in [14,15]. Although concentric cylinder experiments of Prado et al. [14,15] and falling sphere experiments in our study were performed at different pressures (0.1 MPa and 200–500 MPa, respectively), the data are in very good agreement, implying that pressure has minor effect on the viscosity of float glass. In the high temperature range as well, the viscosity of the melt decreases strongly with the addition of water. By adding 3.50 wt% H_2O to the dry melt, the viscosity at 1523 K decreases more than one order of magnitude from 50 Pa s to 3.5 Pa s.

3.4. Pressure effect on viscosity

The pressure effect on viscosity of water-bearing float glass is expected to be small for a composition with an intermediate degree of depolymerization such as float glass [40]. Fig. 5(a)–(d) show the pressure effect of viscosity for glasses with different water contents (0.04–2.14 wt% of H_2O) in the low temperature range. In one case (glass containing 0.28 wt% H_2O) measurements were performed at different pressures and temperatures and then from linear regression at each pressure, we have calculated the values of viscosity at three temperatures (806, 834, and 863 K). For three samples the pressure effect on viscosity is negligible. Only the experiment performed at multiple pressures and temperatures yield a measurable pressure dependence of 0.1 log units per 100 MPa.

An insignificant pressure effect is indicated also for the low viscosity range. Falling sphere experiments with melts containing ~0.68 wt% at 1523 K and pressures of 200 and 500 MPa agree within 0.07 log units. The overall consistency of the data sets shown in Fig. 5 implies that variations in pressure between 0.1 and 500 MPa have minor effect on melt viscosity. Thus, both in the high viscosity and in the low viscosity range pressure appears to have

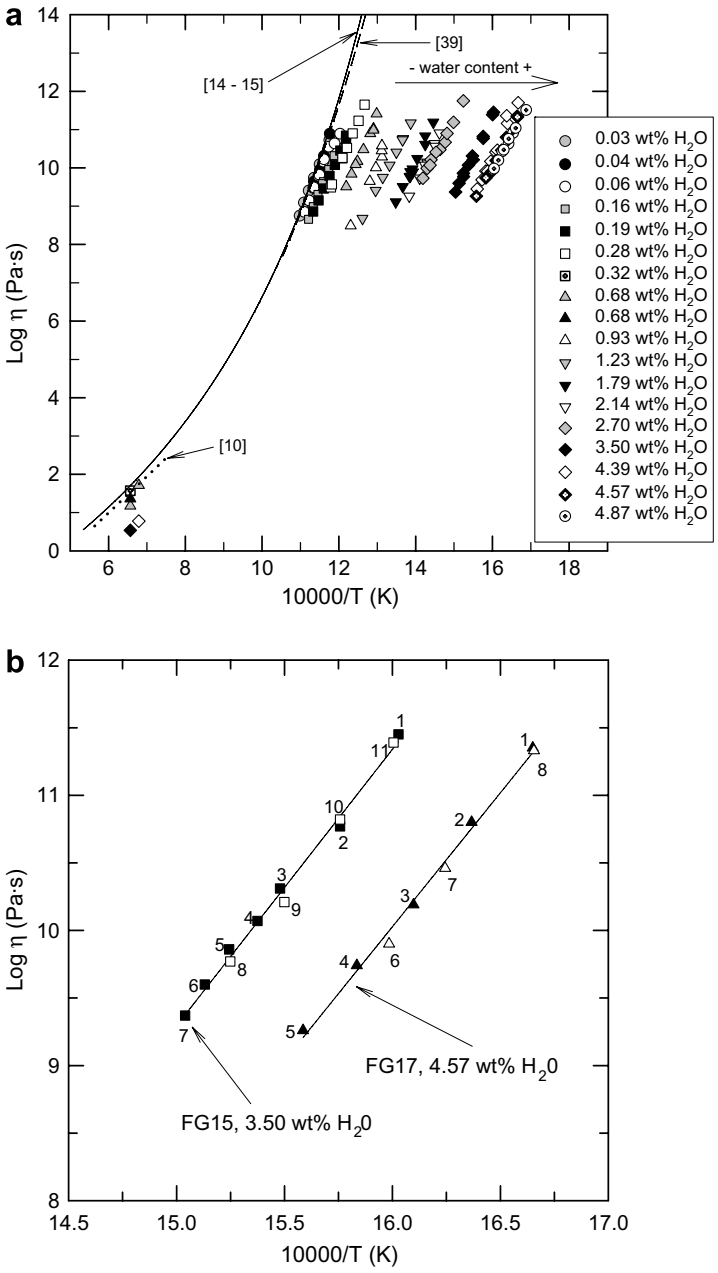

Fig. 3. (a) Compilation of viscosity data for float glass melts in the high and the low viscosity range. Data from literature for dry melts are shown for comparison. (b) Details for two creep experiments. Numbers refer to the sequence in which measurements were performed.

no significant influence on the viscosity of float glass and, hence, high pressure data are directly applicable at ambient pressure as well.

4. Discussion

4.1. Data modeling

Few models are available for prediction of viscosity as function of temperature and water content for silicate melts and no models are known for float glass melt composition. Several empirical approaches were performed to parameterize viscosity of hydrous silicate melts. The first model which allows the prediction of the viscosity of hydrous silicate melts as function of bulk compositions was, to our knowledge, the model of Shaw [41]. The Shaw model considers the viscosity as having Arrhenian behavior. Assuming Arrhenian behavior may be a suitable approach for high temperature melts above the liquidus, but over a wide range of temperature this approach often fails. Therefore, the model of Shaw is limited in application to a narrow viscosity range and cannot be extended to the glass transition. Further models were proposed for specific compositions (e.g. [3,16,17,21,22]) which use an extended version of the VFT equation to take into account the non-Arrhenian behavior of viscosity as function of temperature. Zhang

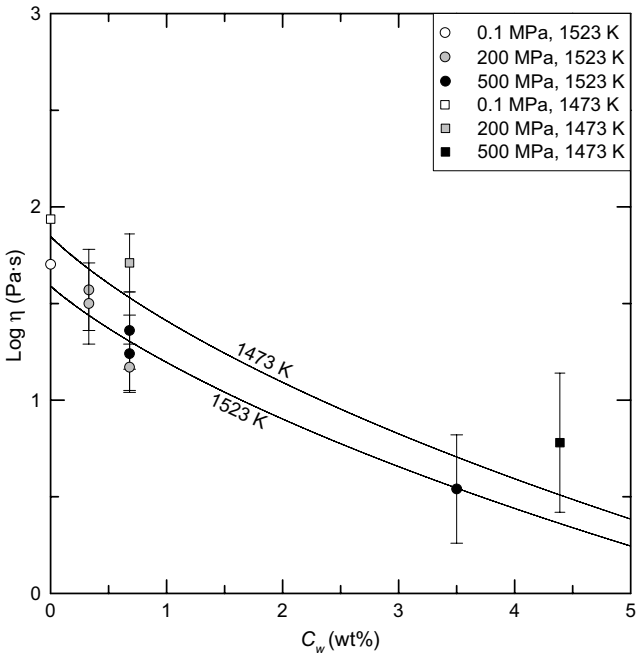

Fig. 4. Results of falling sphere experiments with hydrous float glass melts in comparison with predictions from [14,15] for nominally dry melts (open symbols are for literature data and full symbols for our data). Squares are data at 1473 K, dots are data at 1523 K. Lines show the prediction of our calculation model at two different temperatures.

et al. [23] proposed a power law model for prediction of the viscosity of rhyolitic hydrous melts as function of temperature and water content (as molar fraction). These approaches reproduce quite well the viscosity in a well defined range of temperatures and water contents for a well defined composition but may fail for other compositions.

In order to develop a model to predict the viscosity of hydrous float glass, several types of equations for viscosity were tested. 200 viscosity data were available in total, including data from this study, mainly at 200 MPa but ranging between 50 and 500 MPa, and data at ambient pressure from [10,14,15,42]. The input data cover a viscosity range from $10^{0.5}$ to $10^{11.5}$ Pa s, a temperature range from 593 to 1523 K and a water content range from 0 to 4.87 wt%. Except for one power law model, all the equations tested were VFT-equations modified by introducing a second term containing both the temperature T and the water concentration C_w. The best results though, are obtained using Eq. (6) which is the result of fitting all the data simultaneously without constraining the VFT-parameters in the first term.

$$\log\eta = -3.42 + \frac{5154.4}{(T-495.4)} - \frac{1423.1}{(T-501.8)} \cdot \frac{C_w}{\left(C_w^{0.6053} - 2.6442 + 0.0034\cdot T\right)}, \quad (6)$$

where η is the viscosity in Pa s, T is the temperature in K, and C_w is the H_2O content in wt%. Eq. (6) reproduces all experimental data within a standard error (1σ) of 0.22 log units (Fig. 6). Pressure was not considered in the fit approach, but as pressure effect was found to be small to negligible, Eq. (6) may be applied over the pressure range 0.1–400 MPa without significant error.

For a dry melt the second term is zero and Eq. (6) reduces to a simple VFT. Difference of the parameters to those given by Prado et al. [14,15] ($A = -2.70$, $B = 4358.44$ K, and $T_0 = 533$ K) for the dry melt are due to our extended data set including water-rich samples. To improve fitting of viscosity at low and high temperatures it was required to introduce a temperature dependent expression in the last term of the Eq. (6). As a consequence, however, the model cannot be applied at temperatures lower than T_g (no viscosity data are available to constrain the fit for these temperatures). At very low temperature the calculated curves undergo an inflection and the calculation predicts even a decreasing viscosity with decreasing temperature (dashed curves in Fig. 7). The inflection is at the lowest viscosity for intermediate water contents around 1 wt%. For water-poor and water-rich melts the inflection point is far beyond the experimental range. The high T limits of the melt viscosity (parameters A of the VFT equation) are close to the value proposed by [43] as a general value for silicate melts (-4.30 ± 0.74). Temperature at which viscosity becomes infinite (parameter C) and the pseudoactivation energy associated with the viscous flow (parameter B) are also consistent with previous calculations [43].

4.2. Effect of water content on melt viscosity

To test how well the dependence of melt viscosity on water content is reproduced by the new model, the VFT parameters were determined independently for each sample used in creep experiments using non-linear-least-square method. In order to improve the fitting of melts for which low viscosities were not measured, the low viscosities of these melts were calculated at 1523, 1473, and 1273 K using Eq. (6) and the calculated values were included in the data set for fitting the individual VFT parameters. The interpolated and extrapolated data are shown as open symbols in Fig. 8. Deviations of calculated viscosities from the trends are mainly due to scattering in the experimental viscosities, probably due to uncertainties in the water content. At high water content the fit equation appears to overestimate the dependence of η on C_w. Hence, an extrapolation of Eq. (6) toward higher water contents cannot be recommended.

For log viscosity <12 the variation of viscosity with C_w predicted by the model resembles the trends found in previous studies [3,4]. The decrease in viscosity with the addition of water is especially pronounced at low water content and becomes less strong at high water contents.

4.3. Glass transition T_g and reduced glass transition T_g^*

For the comparison of the glass transition temperatures of different compositions as a function of water content, a model for calculation of the reduced glass transitions T_g^*

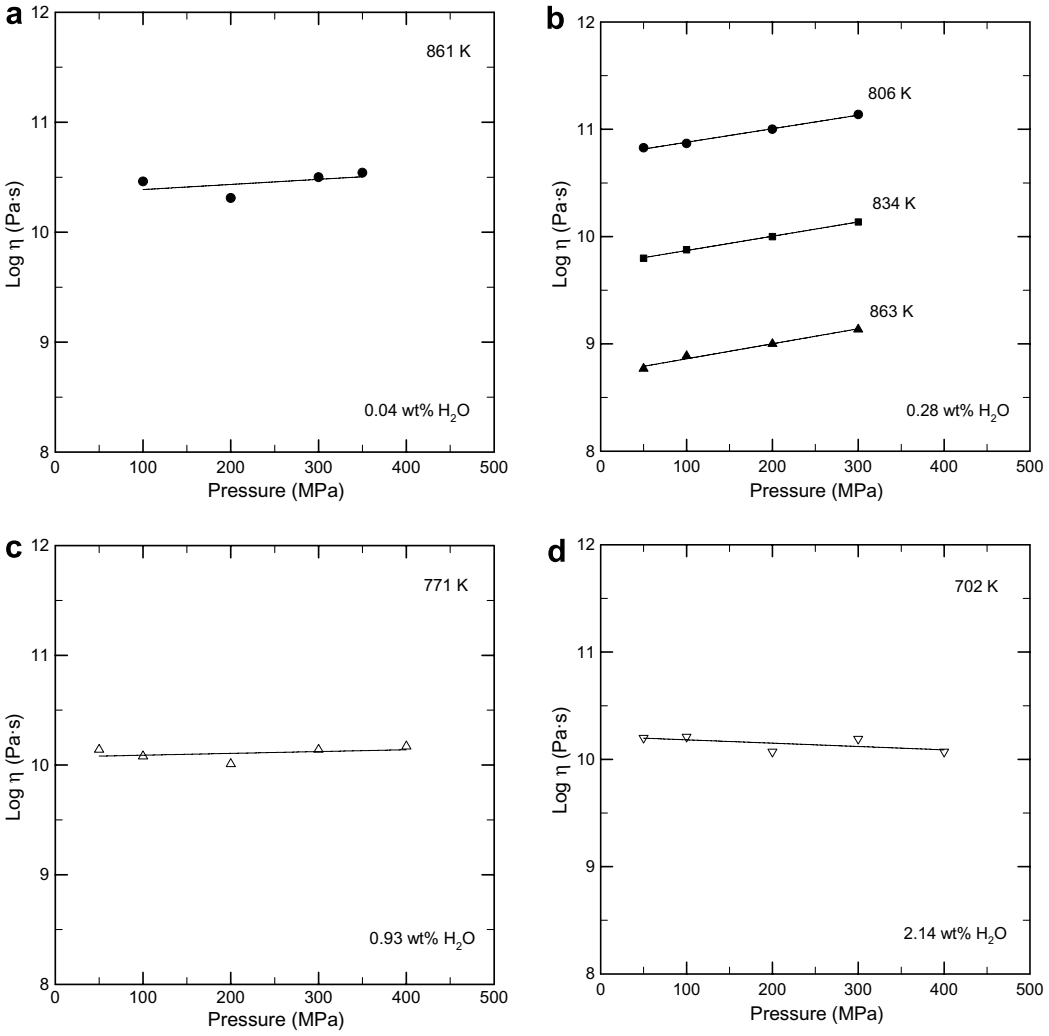

Fig. 5. Effect of pressure on viscosity of float glass melts in the high viscosity range.

was proposed by Deubener et al. [1] based on the three-components-model of Tomozawa et al. [28]. The reduced glass transition T_g^* equals T_g/T_g^{GN} where T_g^{GN} is T_g for the melt containing 0.02 wt% of total water. The model predicts the T_g^* of water-bearing glasses as a weighted combination of contributions of the dry glass, OH groups, and molecular water.

$$T_g^* = \frac{1.01 \cdot C_G + 0.22 \cdot A \cdot C_{OH} + 0.22 \cdot B \cdot C_{H_2O}}{C_G + A \cdot C_{OH} + B \cdot C_{H_2O}}. \quad (7)$$

C_G, C_{OH}, and C_{H_2O} are the corresponding weight fractions of anhydrous glass and water dissolved as OH groups and H_2O molecules. A and B are calculated parameters weighting the influence of hydroxyl and molecular water on the reduced glass transition, respectively. These parameters were proposed in [1] to vary linearly with the number of non-bridging oxygens per tetrahedral cations, NBO/T as $A = 35 - 7.58 \cdot (\mathrm{NBO}/T)$ and $B = 7 - 3.03 \cdot (\mathrm{NBO}/T)$.

In Fig. 9 the values of T_g^* based on the individual VFT parameters in Table 5 are compared to the predictions of [1]. The glass transition of the float glass containing 0.02 wt% of H_2O is 822 K. We did not use Eq. (6) to calculate T_g^* because of the problems associated with the inflection points in particular for intermediate water contents, see above.

Consistent with the model [1] the new data show that the reduced glass transition decreases with the increasing of the total water especially for low water content where total water is mainly dissolved as hydroxyl groups. The effect of total water content has less effect on the T_g^* for water-rich melts where molecular water becomes dominant. Although the general trend is similar, systematic differences between the experimental and the predicted values are evident. At $C_w < 0.68$ wt% the experimental data are below the predictions of [1] while at higher water contents the trend inverses. But the deviations are still within the quoted error of T_g of ±40 K (maximum deviation of 36 K for FG14 containing 2.70 wt% H_2O).

Using data on water speciation in float glass from Table 1 or, for those compositions not measured by IR, from [6] we have re-calculated the parameters A and B by fitting all the T_g^* to Eq. (7). The derived parameter A, weighting the

Please cite this article in press as: P. Del Gaudio et al., Viscosity and glass transition temperature of hydrous float glass, J. Non-cryst. Solids (2006), doi:10.1016/j.jnoncrysol.2006.11.009

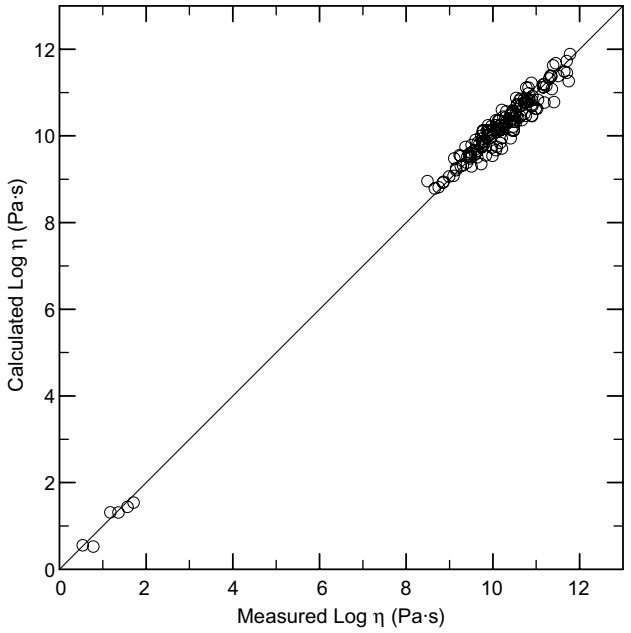

Fig. 6. Comparison between experimental viscosity data and predictions by the new model.

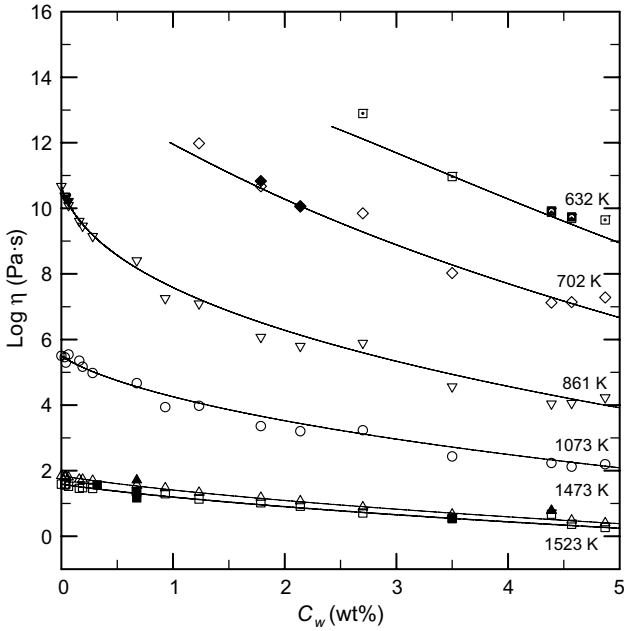

Fig. 8. Viscosity isotherms for hydrous float glass melts. Solid lines are predictions by the model. Filled symbols indicate measured viscosity data. Open symbols refer to viscosities interpolated by using the VFT equations presented in Table 5.

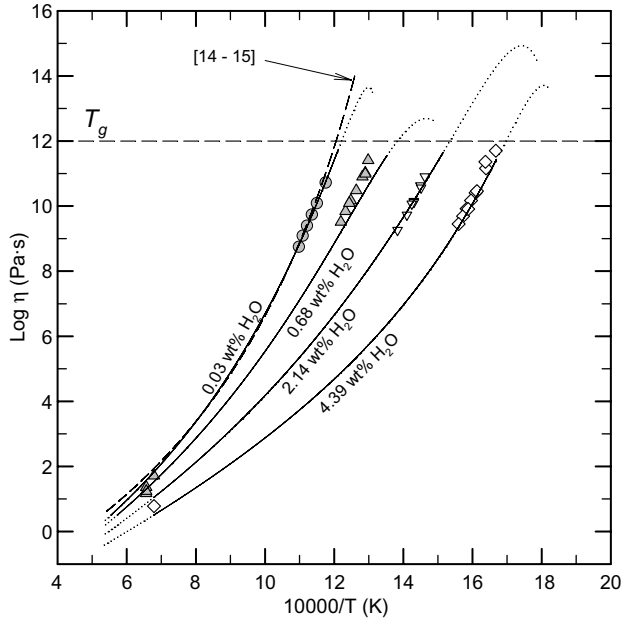

Fig. 7. Arrhenius-plot of the viscosity of float glass melts for four different water contents. Data from [14,15] are shown as dashed lines for comparison. Solid and dotted lines illustrate the predictions of the new model. Note that the model shows artificial trends above 10^{12} Pa s, in particular for intermediate water contents.

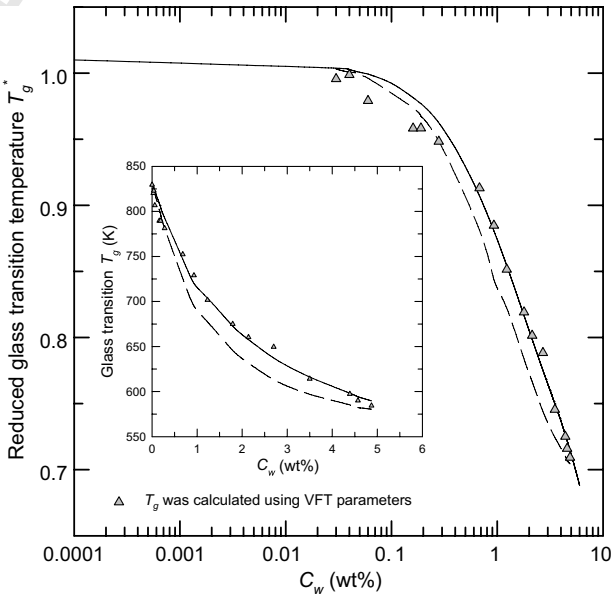

Fig. 9. Reduced glass transition temperatures for float glass melts as a function of water content. The dashed line represents the prediction of [1] with $A = 30$ and $B = 5$. The solid line corresponds to the predictions of T_g^* calculated using the parameters $A = 22.9 \pm 1.1$ and $B = 6.9 \pm 0.8$ fitted to the T_g derived from VFT parameters and water speciation data.

influence of hydroxyl groups, was 22.9 ± 1.1 for float glass. Parameter B, weighting the influence of molecular water, was determined as 6.9 ± 0.8. The two parameters, in both cases, are slightly different from the parameters ($A = 30$ and $B = 5$) calculated after [1] for the NBO/T of the float glass composition (0.77) implying that the influence of molecular H_2O on T_g is more pronounced than predicted by the model whereas the influence of OH groups is less pronounced. However, in float glass the influence of OH groups is still 3.5 times larger than the one of molecular water. The result indicates that the influence of water on melt configuration is more complex than covered by a sim-

Table 5
VFT parameters for float glass melts with different water contents.

Sample	C_w (wt%)	A	B	T_0 (K)
[a]	0.00	−3.42 (0.15)	5154 (188)	495 (10)
FG0a	0.03	−3.68 (0.19)	5536 (258)	467 (13)
FG1	0.04	−2.99 (0.50)	4634 (620)	513 (33)
FG2	0.06	−4.57 (0.59)	6908 (858)	389 (40)
FG3	0.16	−4.66 (0.61)	7115 (915)	362 (42)
FG4	0.19	−3.91 (0.16)	5993 (234)	413 (12)
FG6	0.28	−3.59 (0.13)	5543 (172)	425 (9)
FG9	0.68	−3.75 (0.46)	5803 (689)	384 (35)
FG10	0.93	−2.27 (0.45)	3785 (549)	463 (33)
FG11	1.23	−3.35 (0.12)	5212 (171)	362 (9)
FG12	1.79	−2.42 (0.24)	3844 (293)	408 (18)
FG13	2.14	−2.54 (0.24)	3921 (314)	390 (19)
FG14	2.70	−3.47 (0.21)	5014 (288)	325 (15)
FG15	3.50	−2.34 (0.12)	3287 (127)	385 (8)
FG16	4.39	−1.62 (0.23)	2556 (203)	409 (13)
FG17	4.57	−2.37 (0.11)	3153 (130)	370 (8)
FG18	4.87	−2.91 (0.12)	3792 (159)	330 (9)

Notes: 1 sigma errors of parameters are given in parenthesis.

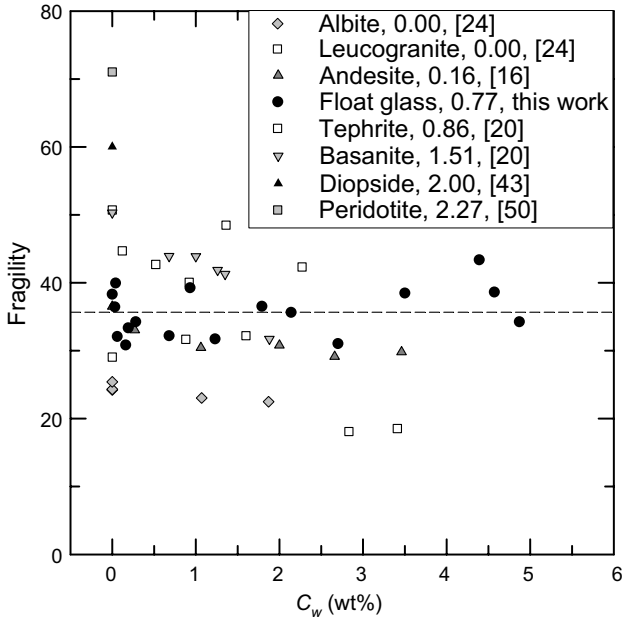

Fig. 10. Fragility of glasses as a function of water content. Selected data from literature are shown for comparison. NBO/T is given behind the sample name.

ple parameter such as the NBO/T ratio. Additional effects may be imposed by interaction of water species with other network ions. For instance the redox state of the melt can change upon hydration. A change of the Fe^{2+}/Fe^{3+} ratio may cause superimposed effects on melt viscosity [44]. However, the iron concentration of the used float glass was low (0.1 wt%) and gradual reduction of the viscosity with increasing Fe^{2+}/Fe^{3+} ratio is assumed to be small. Also an interaction of water with other volatiles, i.e. sulphur species (fining agent), may have some effects on the melt rheology. Further, interaction of protons with sodium ions are discussed to contribute to the mixed alkali effect in glass, which cause a deviation from the expected linear trend of the isokom temperatures in the glass transition range [45].

4.4. Fragility

The fragility is an important parameter describing the dependence of viscosity on temperature. Fragility of glasses was calculated according to [46]. The definition of fragility as the gradient of the viscosity curve at the glass transition temperature on a reduced temperature scale [47,48] is commonly used and has been found to be one of the most satisfactory ones [49]. When using VFT equation the fragility can be expressed as

$$m = \frac{B}{T_g\left(1-\frac{T_0}{T_g}\right)^2},$$

where B and T_0 are VFT parameters. In Fig. 10 we have plotted the fragilities of different compositions, ranging from highly polymerized melt (Albite [24]) to highly depolymerized melt (Peridotite [50]). The fragility of dry glasses strongly increases with depolymerization. For water-bearing melts trends of the fragility parameter m versus C_w are difficult to extract. Several data sets (for albite [24], leucogranite [24], andesite [16], basanite [20]) indicate slight decrease of m with growing water content which contrasts to the dependence of m on melt depolymerization observed for anhydrous melts. Data for tephrite [20] show too large scatter to derive any trend. For float glass composition m seems firstly to decrease with C_w and then at higher m values to increase. However, the change in m (if it exists) is small compared to the scatter of data. It is noteworthy that the change in NBO/T induced by incorporation of water in the melt is small compared to the range of NBO/T covered by the anhydrous compositions shown in Fig. 10. In the case of float glass at most 1.5 wt% of water is dissolved as OH groups [6]. Assuming that OH groups are equivalent to non-bridging oxygens, NBO/T increases only from 0.77 to 0.91. Such increase in NBO/T would increase the fragility of anhydrous melts by not more than 3.

5. Conclusion

The investigation of Newtonian viscosities of hydrous float glass (0.03–4.87 wt% of total water content) over a wide range of temperatures (573–1523 K) and pressure (50–500 MPa) shows that melt viscosity is mainly controlled by temperature and H_2O content of the melt. No significant pressure effect on viscosity was found in quasi-dry (0.03 wt%) and water-bearing float glasses (2.14 wt%) above the glass transition temperature in the pressure range 50–400 MPa, consistent with results of melts having similar molar fraction of non-bridging oxygen ($X_{NBO} = 0.15$) [40]. No variation of viscosity, due to the pressure, at 1523 K and change in pressure from 200 to 500 MPa was found.

In order to calculate viscosities of water-bearing float glass as function of temperature and H_2O content a new

model is presented, applicable in the temperature range from T_g to 1523 K and H_2O – range 0–4.87 wt%. Using this model over the stated range viscosities can be predicted to within 0.22 log units (1σ).

Using water speciation data based on IR spectroscopy, the new viscosity data show that the effect of hydroxyl groups on the glass transition of float glass is much larger than that of dissolved H_2O molecules. The difference in efficiency of both hydrous species is, however, smaller than predicted by the model of [1]. This might reflect that composition plays a more complex role in glass transition than expressed by the simple parameter NBO/T.

Acknowledgments

This work was supported by the German Science foundation, DFG. The authors thank two anonymous reviewers for very constructive comments.

References

[1] J. Deubener, R. Müller, H. Behrens, G. Heide, J. Non-Cryst. Solids 330 (2003) 268.
[2] K.U. Hess, D.B. Dingwell, S.L. Webb, Am. Mineral. 80 (1995) 297.
[3] K.U. Hess, D:B. Dingwell, Am. Mineral. 81 (1996) 1297.
[4] F. Vetere, H. Behrens, F. Holtz, D.R. Neuville, Chem. Geol. 228 (2006) 233.
[5] E.M. Stolper, Geochim. Cosmochim. Acta 46 (1982) 2609.
[6] A. Stuke, H. Behrens, B.C. Schmidt, R. Dupree, Chem. Geol. 229 (2006) 64.
[7] S.L. Webb, D.B. Dingwell, J. Geophys. Res. 95 (1990) 15695.
[8] H. Behrens, M. Nowak, Phase Transit. 76 (2003) 45.
[9] M. Nowak, H. Behrens, Earth Planet. Sci. Lett. 184 (2001) 515.
[10] R. von Euler, G.F. Winkler, M. Lahn, Glastech. Ber. Glass Sci. Technol. 30 (1957) 325.
[11] N. Böse, G. Klingenberg, G. Meerlender, Glastech. Ber. Glass Sci. Technol. 74 (2001) 115.
[12] P. Manns, R. Brückner, Glastech. Ber. 61 (1988) 46.
[13] R. Brückner, G. Demharter, Glastech. Ber. 48 (1975) 12.
[14] M.O. Prado, C. Fredericci, E.D. Zanotto, J. Non-Cryst. Solids 331 (2003) 145.
[15] M.O. Prado, C. Fredericci, E.D. Zanotto, J. Non-Cryst. Solids 331 (2003) 156.
[16] P. Richet, A.M. Lejeune, F. Holtz, J. Roux, Chem. Geol. 128 (1996) 185.
[17] F. Schulze, H. Behrens, F. Holtz, J. Roux, W. Johannes, Am. Mineral. 81 (1996) 1155.
[18] C. Romano, B.T. Poe, V. Mincione, K.U. Hess, D.B. Dingwell, Chem. Geol. 174 (2001) 115.
[19] C. Romano, D. Giordano, P. Papale, V. Mincione, D.B. Dingwell, M. Rosi, Chem. Geol. 202 (2003) 23.
[20] A. Whittington, P. Richet, F. Holtz, Geochim. Cosmochim. Acta 64 (2000) 3725.
[21] D. Giordano, C. Romano, P. Papale, D.B. Dingwell, Chem. Geol. 213 (2004) 49.
[22] F. Holtz, J. Roux, S. Ohlhorst, H. Behrens, F. Schulze, Am. Mineral. 84 (1999) 27.
[23] Y.X. Zhang, Z.J. Xu, Y. Liu, Am. Mineral. 88 (2003) 1741.
[24] A. Whittington, P. Richet, H. Behrens, F. Holtz, B. Scaillet, Trans. Roy. Soc. Edin.: Earth Sci. 95 (2003) 59.
[25] R.F. Bartholomew, B.L. Butler, H.L. Hoover, C.K. Wu, J. Am. Ceram. Soc. 63 (1980) 481.
[26] H. Behrens, A. Stuke, Glastech. Ber. Glass Sci. Technol. 76 (2003) 176.
[27] A. Whittington, P. Richet, Y. Linard, F. Holtz, Chem. Geol. 174 (2001) 209.
[28] M. Tomozawa, M. Takata, J. Acocella, E.B. Watson, T. Takamori, J. Non-Cryst. Solids 56 (1983) 343.
[29] H. Scholze, Glastechn. Ber. 32 (1959) 81.
[30] F. Schulze, H. Behrens, W. Hurkuck, Am. Mineral. 84 (1999) 1512.
[31] D. Neuville, P. Richet, Geochim. Cosmochim. Acta 55 (1991) 1011.
[32] A.N. Gent, Brit. J. Appl. Phys. 11 (1960) 165.
[33] R. Siewert, H. Büttner, M. Rosenhauer, N. Jahrb. Min. Abhandl. 172 (1998) 259.
[34] J. Akella, J. Ganguly, R. Grover, G. Kennedy, J. Phys. Chem. Solids 34 (1973) 631.
[35] J.D. Dudley, H.T. Hall, Repr. Phys. Rev. 118 (1960) 1211.
[36] R.A. Lange, Rev. Mineral. 30 (1994) 331.
[37] F.A. Ochs, R.A. Lange, Science 283 (1999) 1314.
[38] J. Koepke, H. Behrens, Geochim. Cosmochim. Acta 65 (2001) 1481.
[39] A.I. Priven, Glass Phys. Chem. 27 (2001) 527.
[40] H. Behrens, F. Schulze, Am. Mineral. 88 (2003) 1351.
[41] H.R. Shaw, Am. J. Sci. 272 (1972) 870.
[42] M. Thies, PhD thesis, Technischen Universität Berlin, Germany, 2002.
[43] J.K. Russell, D. Giordano, D.B. Dingwell, Am. Mineral. 88 (2003) 1390.
[44] C. Liebske, H. Behrens, F. Holtz, R. Lange, Geochim. Cosmochim. Acta 67 (2003) 473.
[45] S. Zietka, J. Deubener, H. Behrens, R. Müller, Eur. J. Glass Sci. Technol. B, submitted for publication.
[46] M.J. Toplis, D.B. Dingwell, K.U. Hess, T. Lenci, Am. Mineral. 82 (1997) 979.
[47] D.J. Plazek, K.L. Ngai, Macromolecules 24 (1991) 1222.
[48] R. Böhmer, C.A. Angell, Phys. Rev. B 45 (1992) 10091.
[49] K.U. Hess, PhD thesis, Universität Bayreuth, Germany, 1996.
[50] D.B. Dingwell, P. Courtial, D. Giordano, A.R.L. Nichols, Earth Planet. Sci. Lett. 226 (2004) 127.